JOURNAL OF GEOPHYSICAL RESEARCH, VOL. 103, NO. A12, PAGES 29,697–29,704, DECEMBER 1, 1998

Kinetic properties of solar wind minor ions and protons measured with SOHO/CELIAS

S. Hefti,[1,2] H. Grünwaldt,[3] F. M. Ipavich,[4] P. Bochsler,[1] D. Hovestadt,[5] M. R. Aellig,[1] M. Hilchenbach,[3] R. Kallenbach,[1,6] A. B. Galvin,[7] J. Geiss,[8] F. Gliem,[9] G. Gloeckler,[4,10] B. Klecker,[5] E. Marsch,[3] E. Möbius,[7] M. Neugebauer,[11] and P. Wurz[1]

Abstract. Using observations of the Charge Time-of-Flight(CTOF) charge and mass spectrometer of the Charge, Element and Isotope Analysis System (CELIAS), and of CELIAS/proton monitor on board the Solar and Heliospheric Observatory (SOHO), we present an overview of speeds and kinetic temperatures of minor ions and protons in the solar wind near solar minimum, covering the Carrington Rotations 1908 to 1912. In the case of a collision-dominated solar wind the speed of minor ions is expected to be lower or equal to the speed of the protons, and all species are expected to have equal temperatures. On the other hand, minor ions can be accelerated and heated by wave-particle interaction. In this case, equal thermal speeds of all species are expected. CTOF data allow the determination of the kinetic parameters of various ions with high accuracy and with high time resolution. The mean O^{6+} speed of the observed period is $390\,km\,s^{-1}$. The speeds of Si^{7+} and Fe^{9+} correlate well with O^{6+}, the linear correlation coefficient being 0.96 or higher. Our results also indicate that silicon and iron tend to lag behind oxygen with a speed difference of $\sim 20\,km\,s^{-1}$ at $500\,km\,s^{-1}$. At the same time, the kinetic temperature of the ions under investigation exhibit the well-known mass proportionality, which is attributed to wave-particle interactions. During the period of low solar activity in consideration, many cases are observed where the kinetic temperature is extraordinarily low (10^4 K for O^{6+}).

1. Introduction

In order to understand the acceleration process and also the expansion of the solar wind, the kinetic properties of minor ions are of major interest. Because of their low densities, the minor components of the solar wind cannot influence the dynamics of the wind. They can therefore be considered as probes convected with the plasma which carry valuable information about its origin and local properties in the acceleration region of the solar wind.

In a collisionally dominated plasma, one would expect equal speeds of all ions. It has been pointed out that Coulomb collisions with protons actually play a dominant role in the acceleration of minor ions with protons [*Geiss et al.*, 1970]. According to this theory, heavy ions are accelerated by Coulomb drag because of the protons. In this case the speed of heavy ions is expected to be less than or equal the proton speed.

However, often a He^{2+} bulk speed is observed which exceeds the proton speed. *Marsch et al.*, [1982] have explained the observed speed difference between He^{2+} and H^+ by the acceleration of He^{2+} by Alfvén waves carried by the protons. In this wave-particle interaction the temperature of heavy ions is changed as well. Instead of equal temperatures, as expected in the case of a Coulomb collision-dominated plasma with energy equipartition, minor ions are expected to have equal thermal speeds.

In fact, a mass proportional kinetic temperature is often observed in the solar wind [*Ogilvie et al.*, 1980].

[1]Physikalisches Institut, Universität Bern, Bern.
[2]Now at Department of Atmospheric, Oceanic and Space Sciences, University of Michigan, Ann Arbor.
[3]Max-Planck-Institut für Aeronomie, Lindau, Germany.
[4]Space Physics Department, University of Maryland, College Park.
[5]Max-Planck-Institut für extraterrestrische Physik, Garching, Germany.
[6]Now at International Space Science Institute, Bern.
[7]Space Physics Department, University of New Hampshire, Durham.
[8]International Space Science Institute, Bern.
[9]Institut für Datenverarbeitungsanlagen, Technische Universität Braunschweig, Germany.
[10]Also at Department of Atmospheric, Oceanic and Space Sciences, University of Michigan, Ann Arbor.
[11]Jet Propulsion Laboratory, Pasadena, California.

Paper number 1998JA900022.
0148-0227/98/1998JA900022$09.00

In this paper we present measurements of the kinetic properties of minor ions and protons performed with the Charge, Element and Isotope Analysis System (CELIAS) on board the Solar and Heliospheric Observatory (SOHO). We find that O^{6+} usually has a higher bulk speed than the protons, as has been observed before for He^{2+} [*Marsch et al.*, 1982]. However, our results also indicate that silicon and iron ions tend to lag behind the protons. We confirm that collisional coupling to protons, as expressed by the kinetic temperature of the ions, depends on m/q^2 of the ion species.

2. Instrument

The charge time-of-flight (CTOF) sensor is part of the Charge, Element, and Isotope Analysis System (CELIAS) on board the Solar and Heliospheric Observatory (SOHO). The three-axis stabilized spacecraft is positioned at the Lagrangian point L_1 and is an ideal platform for the optical observations of the Sun and for in situ solar wind measurements. CTOF is a charge and mass spectrometer which uses a combination of electrostatic deflection, time-of-flight (TOF) measurement, and energy measurement in a solid state detector to determine the energy, mass per charge m/q, and mass m of solar wind ions. The proton data have been measured by the CELIAS/proton monitor sensor [*Ipavich et al.*, 1998]. CELIAS is a joint effort of five hardware institutions under the direction of the Max-Planck-Institute for Extraterrestrial Physics (Garching, Germany) (prelaunch) and the University of Bern (postlaunch). The Max-Planck-Institute for Aeronomy (Lindau, Germany) was the prime hardware institution for CTOF, the University of Bern provided the entrance system, and the Technische Universität Braunschweig provided the data processing unit. The proton monitor was built at the University of Maryland, USA. The CELIAS instrument is described in detail by *Hovestadt et al.*, [1995].

3. Data Reduction

For each detected ion the CTOF sensor determines the energy per charge E/q, the time-of-flight τ in the sensor, and the energy E_{SSD} deposited in the solid state detector. From these measurements we determine the speed v, the mass per charge ratio m/q, and the mass m of the ion. The data processing unit (DPU) uses a fast algorithm to determine m/q and m for each detected ion and accumulates E/q spectra for the different ion species separately on the basis of this classification, to be called "matrix rates." A total of 508 different regions in the mass per charge and mass domain are used to accumulate 508 E/q spectra per sensor cycle. In this work, we are using only a few of these spectra to demonstrate the instrument capabilities. More ion species will be investigated in the future using the same technique. In order to reduce telemetry load, the E/q spectra are compressed. Two different compression schemes are used depending on the availability of the speed of iron v_{Fe}, which is calculated by the DPU on board. In case the v_{Fe} is determined by the DPU, histograms are generated with good resolution at the expected center of the distribution, but with lower resolution toward the tails ("compressed binning"). In this mode the resolution in the center of the distribution is 6 % in E/q or 3 % in speed. Otherwise, equidistant binning is used, with 21 bins of fixed width. In the latter case the resolution is 15 % in v everywhere in the spectrum.

In both cases the kinetic properties can be determined. We use a fit to the response function of the entrance system to the matrix rates [see *Aellig et al.*, 1998, equation (B3)]. The energy per charge resolution of the entrance system is taken into account by the response function.

We selected a period of cold solar wind to demonstrate the correctness of the data reduction method. During periods of cold solar wind the peak of O^{6+}, normally hidden in the shoulder of He^{2+}, is visible in the "start rate" spectra. The start rate is a measure of the number of ions passing the entrance system at each E/q step. Start rate spectra can therefore be used to determine kinetic properties in a straightforward manner, as it has been done for the very first solar wind experiments [e.g.,*Bame et al.*, 1975].

Figure 1 shows a histogram of the start rate as a function of E/q for one sensor cycle. The E/q has been

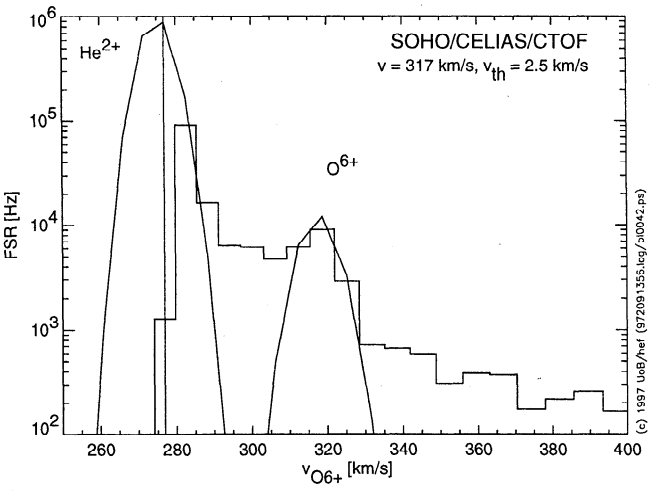

Figure 1. CTOF start rate (FSR) for a particular case of cold solar wind collected during day 210.0 of year 1996. The E/q scale has been converted to v_{O6+}. In this spectrum the peak of O^{6+} is clearly visible and can be used to verify the kinetic parameters of this ion derived from the matrix rates. This is indicated by the parabola-shaped curves, which show peaks calculated from the kinetic properties derived with our data reduction method. The vertical line at $v = 274\,\mathrm{km\,s^{-1}}$ indicates the location of the step reversal. The energy per charge resolution of the entrance system of the sensor has been taken into account to determine the kinetic temperature.

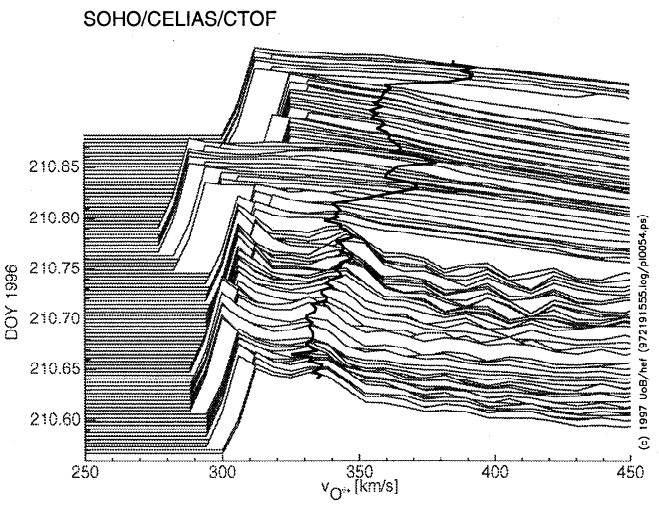

Figure 2. Stack plot of the CTOF start rate on day 210 of 1996. The z axis is logarithmically scaled. During the first half of the period the O^{6+} peak is visible in the start rate. Then the thermal speed of the solar wind increases from one spectrum to the next, that is, within 5 min, and O^{6+} is no longer visible because of overlap of He^{2+}. Indicated by the bold solid line is the O^{6+} speed as derived with our data reduction method using the matrix rates. With the mass and mass per charge information available the O^{6+} speed can still be determined.

converted to the speed of O^{6+}. The spectrum usually is truncated due to "step reversal" (The downstepping in E/q has been stopped at count rates exceeding a given limit in order to avoid damage of the detectors. The spectrum usually is truncated if the start rate exceeds 100 kHz.). Overplotted as parabola-shaped curves is equation (B3) from *Aellig et al.* [1998] for He^{2+} and O^{6+} using the kinetic properties determined from the matrix rates. Clearly, the data reduction method gives correct results for both the speed and the thermal speed. Note that the kinetic temperature of O^{6+} is extremely low in this case ($\sim 10^4$ K). The broadening of the peak due to the energy per charge resolution of the entrance system has been taken into account and does not contribute significantly to the uncertainty of the kinetic temperature.

Figure 2 shows a stack plot of E/q spectra as shown in Figure 1, covering a period of 8 hours. A spectrum is plotted every 5 min; the z axis is logarithmically scaled. During the first half of the shown period the solar wind is cold, and the O^{6+} peak is visible. Then the conditions change from one spectrum to the next, and hot solar wind is observed. The bold line in Figure 2 indicates the speed of O^{6+}, as determined from the matrix rates with our data reduction method. The peak of O^{6+} is always matched by the speed determined form the matrix rates, as can be seen in Figure 2, as long as the solar wind is cold. In case of hot solar wind the kinetic properties of minor ions cannot be determined from the start rate spectra alone, and the mass and mass per charge information must be used. The data reduction procedure is described in further detail in the thesis of *Hefti* [1997].

4. Results

Using the SOHO/CELIAS/CTOF data from Carrington Rotations 1908 to 1912, we have derived the bulk speeds and kinetic temperatures of O^{6+}, Si^{7+}, and Fe^{9+}.

Figure 3a gives an overview of the oxygen bulk speed. The mean speed during the investigated period was $390 \pm 60\,\mathrm{km\,s^{-1}}$, which is typical for solar wind near solar minimum. While the speed was generally low, some high-speed streams were observed occasionally because of coronal holes extending to the equatorial region.

Figure 3b shows a record of the kinetic temperature of O^{6+}. Its mean value was 1.4×10^6 K. During this part of the solar cycle many cases of low kinetic temperature have been observed. Day 210, which we have already discussed above, is one such example with kinetic temperatures of O^{6+} as low as $\sim 10^4$ K.

Figure 4 shows the comparison of bulk speeds of minor ions and protons. The dashed line indicates equal speeds of both ion species, while the solid line shows the result of a linear fit to the observations. We find that the bulk speeds of the different ions as measured at 1 AU agree very well, the linear correlation coefficient being $r = 0.96$ or higher. Note that the speeds of protons and minor ions are determined by two different instruments and are derived completely independently.

Close inspection of the data reveals speed differences between the investigated ions. Oxygen tends to have higher speeds than protons for proton speeds above $350\,\mathrm{km\,s^{-1}}$ (Figure 4a). Below $350\,\mathrm{km\,s^{-1}}$ the speed of O^{6+} is actually lower than the proton speed. In contrast, silicon and iron tend to lag behind oxygen (Figures 4c and 4b). Iron and silicon have basically the same speed (Figure 4d). The slight deviation of iron from silicon in high-speed streams, as indicated in Figure 4, is considered not to be significant, since high-speed solar wind was not often observed during the analyzed period (Figure 3).

Because of the large geometric factor and the 100 % duty cycle of the sensor, the kinetic properties of oxygen, silicon, and iron can be determined from the data of each sensor cycle, that is, with a time resolution of 5 min. This is also important to avoid including speed variations as part of the temperature. The samplings of Fe^{9+} and O^{6+} are $\sim$ 50 s apart due to the downstepping in E/q. We do not expect significant changes in the kinetic properties of minor ions on this timescale. Also, data of the investigated ions can be directly compared since they are measured under exactly the same plasma conditions and with exactly the same time resolution.

It is well known that the helium speed is usually higher than the proton speed at high proton speeds [e.g.,*Marsch et al.*, 1982]. These authors have explained the acceleration of the helium ions by Alfvén waves

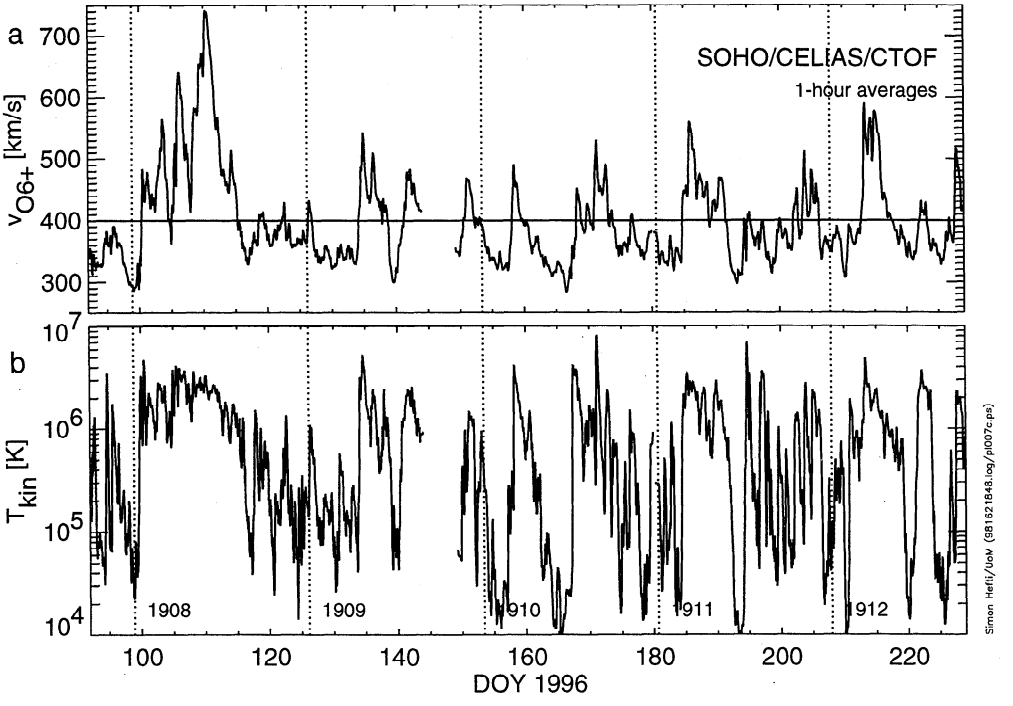

Figure 3. One-hour averages of bulk speed and kinetic temperature of O^{6+} for the Carrington Rotations 1908 to 1912. The mean solar wind speed during this period is 390 km s^{-1}, and only a few high-speed streams are observed, as is typical for solar minimum.

carried by protons. A similar mechanism will cause the oxygen ions to have higher speeds than protons.

In our data set we do not observe such a preferential acceleration for silicon and iron, however. Both ions tend to lag behind oxygen at speeds above 350 km s^{-1} and have similar speeds as the protons. Possibly, these species are actually faster than O^{6+} at lower speeds, but we do not consider this result to be significant, because of the low number of measurements at very low speeds.

Similar observations have been reported earlier by *Bochsler* [1989] and *Schmid et al.*, [1987], who have compared kinetic properties of helium, silicon, and iron as measured with the ion composition instrument (ICI) on the ISEE 3 spacecraft. The authors found that in high-speed streams, silicon and iron speeds were lower than the helium speed.

Our results differ from the observation of *Ipavich et al.* [1986], who reported that the speed of iron was higher than the proton speed by about the Alfvén speed during four periods of fast solar wind, measured with the ULECA instrument on the ISEE 3 spacecraft in 1978. Also, *von Steiger and Geiss* [1995] have not observed such speed differences with the solar wind composition instrument (SWICS) on Ulysses. This raises the question of whether minor ions are still accelerated on their way from 1 AU (ISEE 3 and SOHO) to 5 AU (Ulysses).

A qualitative explanation for the different behavior of minor ions is the ordering of different species according to the ion cyclotron resonance frequency, $\omega_{c,i}$, that is, according to q/m. *Isenberg and Hollweg* [1983] have shown that the acceleration of minor ions by waves is proportional to $(q/m)^{2-\gamma}$, where γ is the spectral index of the wave spectrum. In the case of $\gamma < 2$ the wave action could maintain higher speeds for species with high q/m such as O^{6+}, whereas, according to this scheme, Si^{7+} or Fe^{9+} would relax relatively soon to the proton speed, that is already at the distance of 1 AU, even in coronal hole associated fast solar wind.

Figure 5 shows comparisons of the kinetic temperatures of the investigated ions. Plotted is the logarithm of the kinetic temperature per mass. The dotted line indicates mass proportional temperatures which are expected if wave-particle interaction is important. In the case of a collision dominated plasma, equal temperatures of all ions are expected. This is indicated by the dashed line.

In Figure 5a the temperatures of oxygen and protons are compared. Figure 5a shows that both equal and mass proportional temperatures are observed in the case of oxygen.

A similar result is found for silicon (Figure 5c). As for oxygen, in many cases the mass proportionality of the kinetic temperatures holds. In some cases, the Si^{7+} temperature approaches the proton temperature. Compared to oxygen, this trend to equal temperatures in case of low proton temperatures is less pronounced for silicon.

Figure 5b shows the same data for Fe^{9+}. In most of the cases, proton and iron temperatures are mass proportional. As already noted for silicon, the "tail" toward equal temperatures of protons and iron ions has

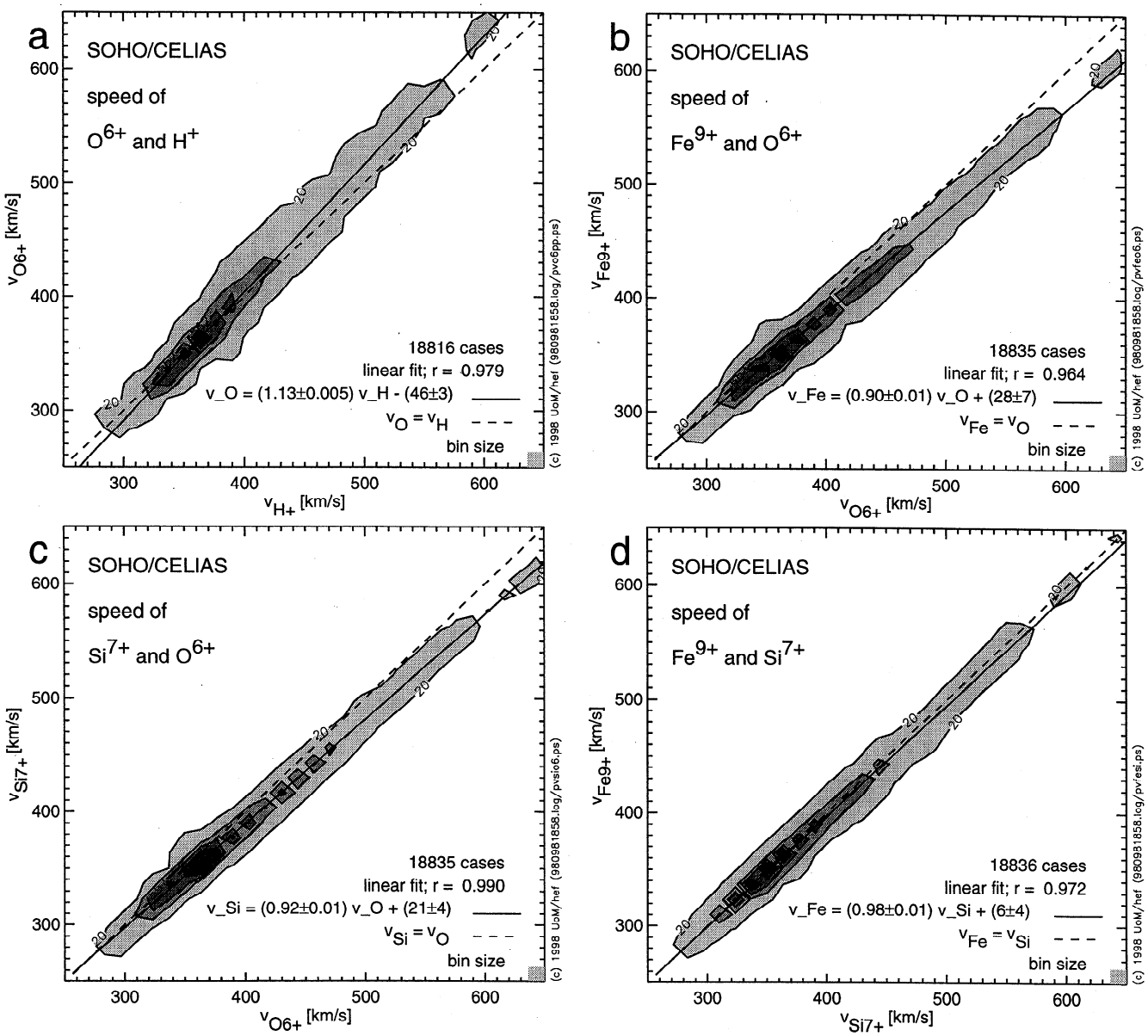

Figure 4. Comparison of the bulk speeds of protons O^{6+}, Si^{7+}, and Fe^{9+}. The dashed lines indicate equal bulk speeds of both ions species, while the solid lines show a linear fit to the data. The bulk speeds of all ions agree remarkably well, the correlation coefficient being 0.96 or higher. While O^{6+} tends to have a higher speed than protons, as expected from acceleration of minor ions by Alfvén waves, both silicon and iron tend to lag behind the protons. Ten-minute averages have been used for Figure 4. Note that because of the excellent count rates of the CTOF sensor, we have $\sim$ 19.000 measurements, even for rare species like Fe^{9+}.

decreased. Silicon and iron usually have the same temperature per mass, as shown in Figure 5d.

This result may be explained by the mass dependent equilibration time τ_{eq}, the time it takes for two ion distributions to equilibrate because of Coulomb collisions. The timescale of collisional coupling of protons and minor ions is given by

$$\tau_{eq} \sim \frac{m_p}{q_p^2}\frac{m_j}{q_j^2}\frac{1}{n_p}\left(\frac{T_p}{m_p}+\frac{T_j}{m_j}\right)^{3/2} \quad (1)$$

where j describes the quantity of the minor ion and n_p is the proton density [*Spitzer*, 1962].

The equilibration time scales with m/q^2. Since $\tau_{eq,O6+} < \tau_{eq,Si7+}$ and $\tau_{eq,Si7+} < \tau_{eq,Fe9+}$, this could explain why equal kinetic temperatures of protons and silicon or iron are less often observed than equal temperatures of protons and oxygen and why equal kinetic temperatures of protons and Fe^{9+} are less often observed than equal temperatures of protons and Si^{7+}.

The presence of Coulomb collisions is even more evident if the equipartition time τ_{eq}, is compared to the expansion time of the plasma, τ_{ex}. If $\tau_{eq} < \tau_{ex}$, the kinetic energy is equilibrated by Coulomb collisions, and equal kinetic temperatures of all ions result. In the case

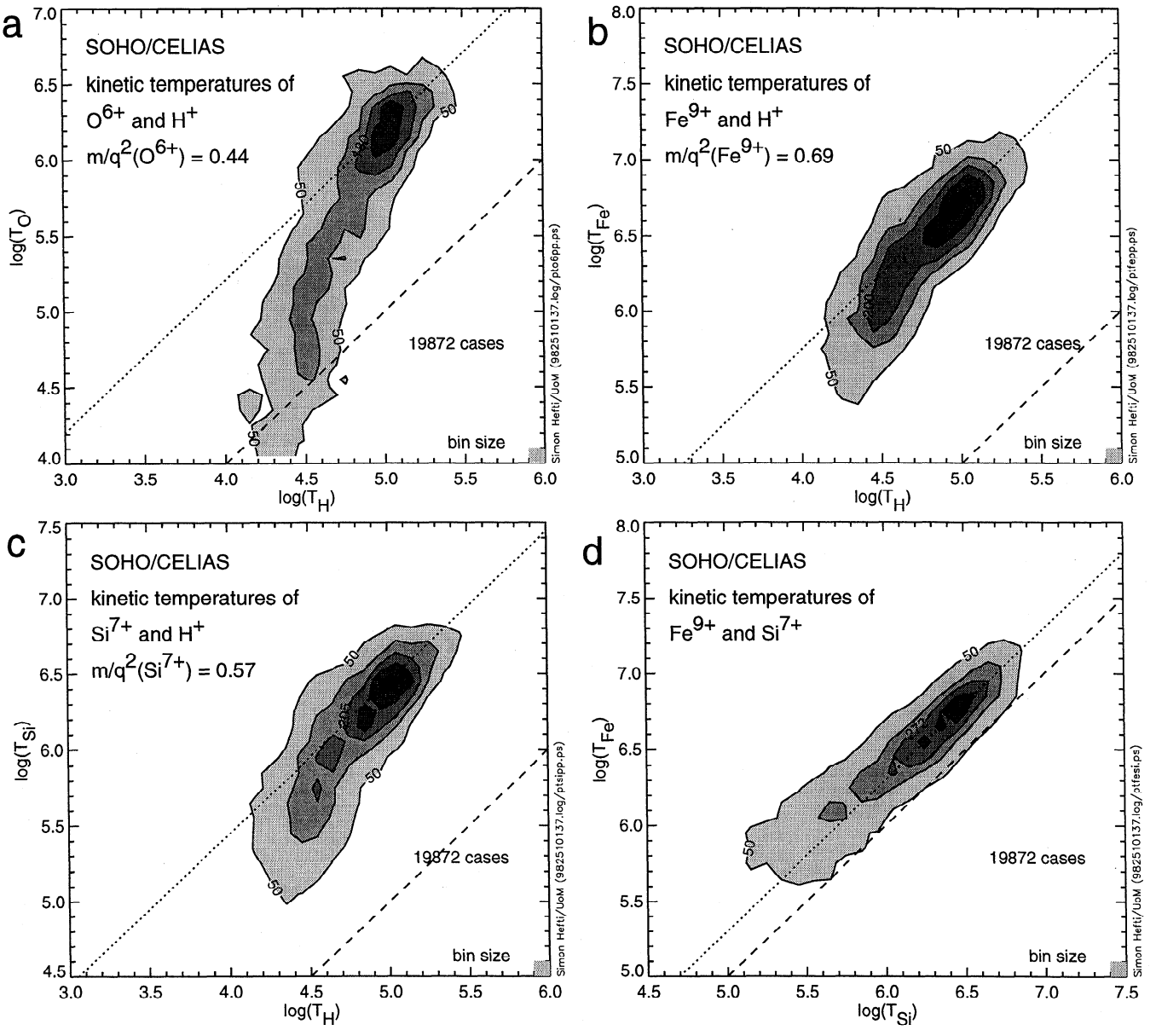

Figure 5. Comparison of the kinetic temperatures of protons O^{6+}, Si^{7+}, and Fe^{9+}. The dotted line indicates equal thermal speeds, or temperatures which scale with mass. The dashed lines show equal temperatures. Clearly, both cases with equal thermal speeds and cases with equal temperatures are observed. The trend toward equal temperatures diminishes with increasing m/q^2. Ten-minute averages have been used for Figure 5. Note that we have $\sim$ 19.000 measurements for all ion species.

of $\tau_{eq} > \tau_{ex}$ the minor ions are not affected by Coulomb collisions, and mass-proportional kinetic temperatures are expected. This is indeed observed.

Using $\tau_{ex} = [v_p\, d\ln n_p/dr]^{-1} \approx 7.5 \times 10^7 R/v_p$, the ratio of equilibration to expansion time is given by

$$\tau_{eq}/\tau_{ex} \approx 3.125 \times 10^{-9} \frac{v_p}{n_p} \left(\frac{T_p}{m_p} + \frac{T_j}{m_j}\right)^{3/2} \quad (2)$$

where v_p is the proton speed in km s^{-1}, n_p is the proton density in cm^{-3}, and R is the heliocentric distance in AU [*Feldman et al.*, 1974].

Figure 6 shows the kinetic temperature ratios versus the ratio (2), as determined from our data, for O^{6+}, Si^{7+}, and Fe^{9+}. Shown are the mean values and the standard deviations in narrow bins of T_j/T_p. Clearly, kinetic temperatures of the minor ions equal the proton temperatures when $\tau_{eq} < \tau_{ex}$, while mass proportional temperatures are observed when the equilibration time is significantly larger than the expansion time.

5. Conclusion

We have presented an overview of the kinetic properties of O^{6+}, Si^{7+}, and Fe^{9+}, measured with SOHO /CELIAS/CTOF, which we have compared with kinetic properties of protons, measured with the SOHO/ CELIAS/proton monitor. The CTOF sensor allows the

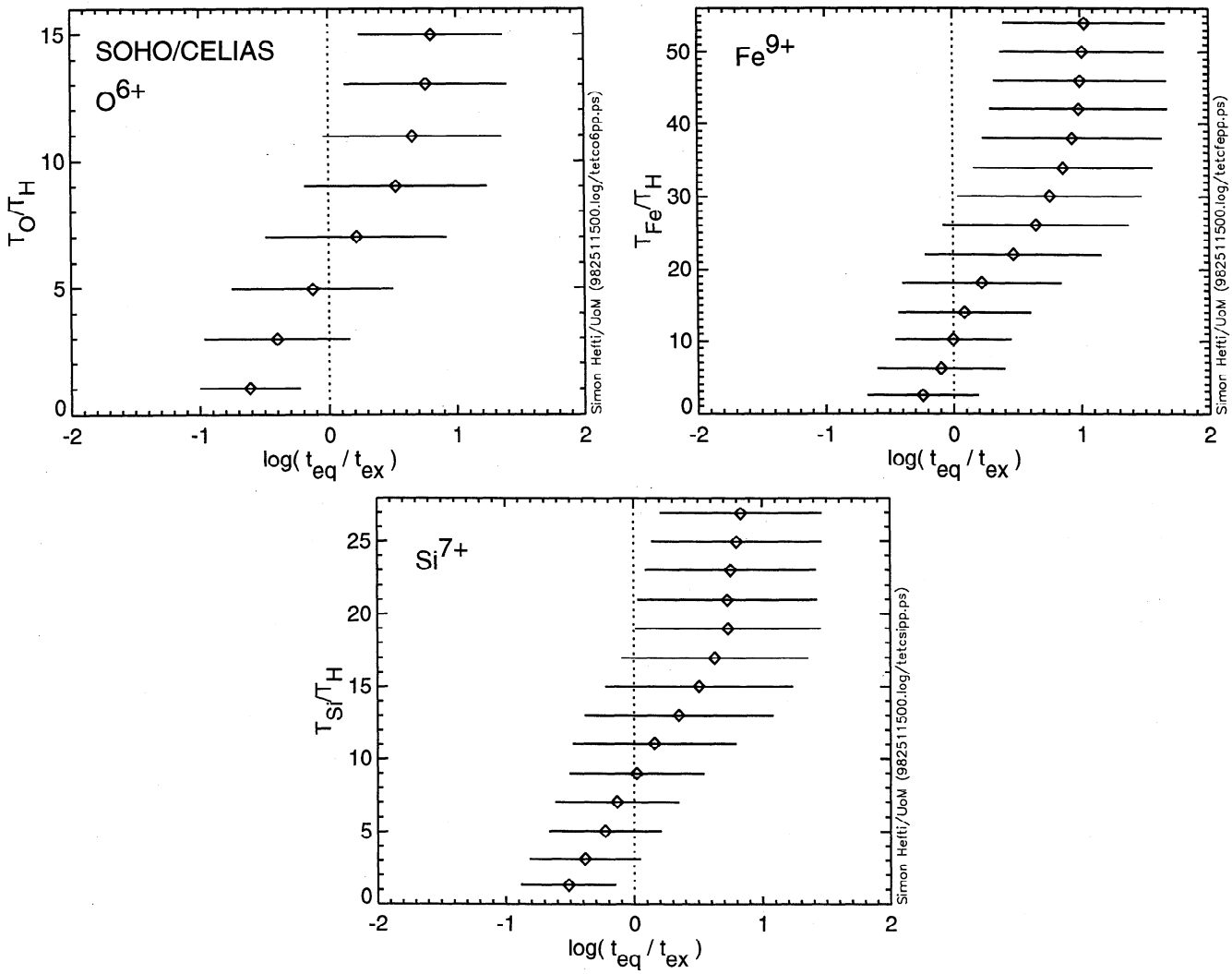

Figure 6. The ratio of the kinetic temperatures of a minor ion and protons versus the ratio of equilibration and expansion time, τ_{eq}/τ_{ex}, for O^{6+}, Si^{7+}, and Fe^{9+}. Shown are the mean and the standard deviation of τ_{eq}/τ_{ex} in narrow bins of T_j/T_{H+}. If the equilibration time, compared to the expansion time, is short, many cases of equal kinetic temperatures of both protons and minor ions are observed. If the equilibration time is longer than the expansion time, Coulomb collisions cannot equilibrate the kinetic energy, and mass-proportional temperatures are observed.

accurate determination of the kinetic properties of minor ions with unprecedented time resolution of 5 min. We have found a good correlation of proton and minor ion speeds. While oxygen ions usually have higher speeds than protons, silicon and iron tend to lag behind oxygen. This result is in contrast to observations made on Ulysses at 5 AU but confirms results based on ISEE 3/ICI measurements made at 1 AU.

The period covered by this analysis is, however, special: The data have been collected during a few months very close to the solar minimum, and they characterize in-ecliptic solar wind. It contains many cases of extremely low kinetic temperatures of minor ions.

We have also investigated the kinetic temperatures of minor ions. The temperatures of the minor ions are usually proportional to the ion mass. In dense plasma a trend toward equal temperatures of minor ions and protons is observed because of collisional coupling. The coupling is strongest for oxygen and less pronounced for silicon and iron. In addition, the coupling of iron to protons is weaker than the coupling of silicon to protons. This is explained by the scaling of the equilibration time with m/q^2. Clearly, the temperature ratio of the minor ions to the protons depends on the ratio of the equilibration and expansion times of the plasma.

Acknowledgments. This work is supported by the Swiss National Science Foundation and by the PRODEX program of ESA. We wish to thank the referees for many comments and suggestions. We also appreciate discussions with R. Wimmer and M. A. Lee.

Janet G. Luhmann thanks Clifford Lopate and another referee for their assistance in evaluating this paper.

References

Aellig, M. R., et al., Iron freeze-in temperatures measured by SOHO/CELIAS/CTOF, *J. Geophys. Res.*, *103*(A8), 17,215 - 17,222, 1998.

Bame, S.J., J.R. Asbridge, W.C. Feldman, M.D. Mont-

gomery, and P.D. Kearney, Solar wind heavy ion abundances, *Sol. Phys.*, *43*, 463-470, 1975.

Bochsler, P., Velocity and abundance of silicon ions in the solar wind, *J. Geophys. Res.*, *94*(A3), 2365-2373, 1989.

Feldman, W.C., J.R. Asbridge, and S.J. Bame, The solar wind He^{2+} to H^{+} temperature ratio, *J. Geophys. Res.*, *79*(16), 2319-2323, 1974.

Geiss, J., P. Hirt, and H. Leutwyler, On acceleration and motion of ions in corona and solar wind, *Sol. Phys.*, *12*, 458-483, 1970.

Hefti, S., Solar wind freeze-in temperatures and fluxes measured with SOHO/CELIAS/CTOF and calibration of the CELIAS sensors, Ph.D. thesis, Univ. of Bern, Bern, 1997.

Hovestadt, D., et al., CELIAS — charge, element and isotope analysis system for SOHO, Sol. Phys. , *162*, 441-481, 1995.

Ipavich, F. M., A. B. Galvin, G. Gloeckler, D. Hovestadt, S. J. Bame, B. Klecker, M. Scholer, L. A. Fisk, and C. Y. Fan, Solar wind Fe and CNO measurements in high-speed flows, *J. Geophys. Res.*, *91*(A4), 4133-4141, 1986.

Ipavich, F. M., et al., Solar wind measurements with SOHO: The CELIAS/MTOF proton monitor, *J. Geophys. Res.*, *103*(A8), 17,205 - 17,213, 1998.

Isenberg, P. A., and J. V. Hollweg, On the preferential acceleration and heating of solar wind heavy ions, *J. Geophys. Res.*, *88*(A5), 3923-3935, 1983.

Marsch, E., K. H. Mühlhäuser, H. Rosenbauer, R. Schwenn and F. M. Neubauer, Solar Wind helium ions: observations of the helios solar probes between 0.3 and 1 AU, *J. Geophys. Res.*, *87*(A1), 35-51, 1982.

Ogilvie, K. W., P. Bochsler, J. Geiss, and M. A. Coplan, Observations of the velocity distribution of solar wind ions, *J. Geophys. Res.*, *85*(A11), 6069-6074, 1980.

Schmid, J., P. Bochsler, and J. Geiss, Velocity of iron ions in the solar wind, *J. Geophys. Res.*, *92*(A9), 9901-9906, 1987.

Spitzer, L., *Physics of Fully Ionized Gases*, 2nd Edition, Wiley-Interscience, New York, 1962.

von Steiger, R. and J. Geiss, Kinetic properties of heavy ions in the solar wind from SWICS/Ulysses, Space Sci. Rev. , *72*, 71-76, 1995.

M. R. Aellig, P. Bochsler, and P. Wurz, Physikalisches Institut, Universitat Bern, Sidlerstrasse 5, CH-3012 Bern, Switzerland. (e-mail: maellig@soho.unibe.ch; bochsler@soho.unibe.ch; wurz@soho.unibe.ch)

A. B. Galvin and E. Möbius, Space Physics Department, University of New Hampshire, Durham, NH 03824. (e-mail: moebius@rotor.sr.unh.edu)

J. Geiss, International Space Sciences Institute, Bern, Switzerland.

F. Gliem, Institut für Datenverarbeitsanlangen, Technische Universitat, D-38023 Braunschweig, Germany. (e-mail: gliem@ida.ing.tu-bs.de)

G. Gloeckler and F. M. Ipavich, Space Physics Department, University of Maryland, College Park, MD 20742. (e-mail: ipavich@umtof.umd.edu)

H. Grünwaldt, M. Hilchenbach, and E. Marsch, Max-Planck-Institut für Aeronomie, D-37189 Lindau, Germany. (e-mail: gruenwaldt@linaxl.dnet.gwdg.de)

S. Hefti, Department of Atmospheric, Oceanic and Space Sciences, College of Engineering, University of Michigan, 2455 Hayward Street, Ann Arbor, MI 48109-2143. (e-mail: hefti@umich.edu)

D. Hovestadt and B. Klecker, Max-Planck-Institut fur Extraterrestrische Physik, D-85740 Garching, Germany.

R. Kallenbach, International Space Science Institute, Bern, Switzerland.

M. Neugebauer, Jet Propulsion Laboratory, Pasedena, CA 91103. (e-mail: mneugeb@jplsp.jpl.nasa.gov)

(Received July 13, 1998; revised September 9, 1998; accepted September 9, 1998.)